ACS APPLIED MATERIALS & INTERFACES

Research Article

www.acsami.org

Boosting the Boron Dopant Level in Monolayer Doping by Carboranes

Liang Ye,[†,‡] Arántzazu González-Campo,[§] Rosario Núñez,[∥] Michel P. de Jong,[‡] Tibor Kudernac,[*,†] Wilfred G. van der Wiel,[‡] and Jurriaan Huskens[*,†]

[†]Molecular NanoFabrication group and [‡]NanoElectronics Group, MESA+ Institute for Nanotechnology, University of Twente, P.O. Box 217, 7500 AE Enschede, The Netherlands

[§]Functional Nanomaterials and Surfaces group and [∥]Inorganic Materials and Catalysis group, Institut de Ciència de Materials de Barcelona (ICMAB-CSIC), Campus de la UAB, 08193, Bellaterra, Spain

Supporting Information

ABSTRACT: Monolayer doping (MLD) presents an alternative method to achieve silicon doping without causing crystal damage, and it has the capability of ultrashallow doping and the doping of nonplanar surfaces. MLD utilizes dopant-containing alkene molecules that form a monolayer on the silicon surface using the well-established hydrosilylation process. Here, we demonstrate that MLD can be extended to high doping levels by designing alkenes with a high content of dopant atoms. Concretely, carborane derivatives, which have 10 B atoms per molecule, were functionalized with an alkene group. MLD using a monolayer of such a derivative yielded up to ten times higher doping levels, as measured by X-ray photoelectron spectroscopy and dynamic secondary mass spectroscopy, compared to an alkene with a single B atom. Sheet resistance measurements showed comparably increased conductivities of the Si substrates. Thermal budget analyses indicate that the doping level can be further optimized by changing the annealing conditions.

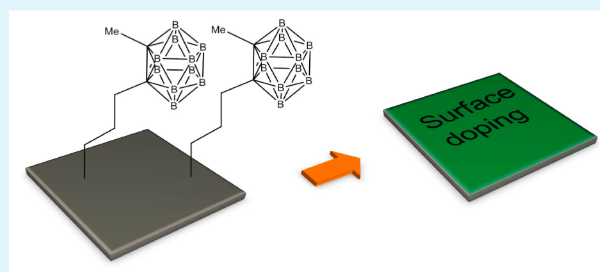

KEYWORDS: *monolayer doping, carboranes, silicon doping, interfaces, hydrosilylation*

INTRODUCTION

Semiconductor technology is continuously pushed toward smaller dimensions in order to achieve better device performance and lower fabrication costs.[1,2] Doping of silicon is one of the crucial steps in semiconductor device fabrication.[3] Doping introduces foreign atoms into the silicon crystal lattice that change the conductivity of the material. Desired electrical properties can be achieved by tuning the concentration or nature of these dopant atoms. Conventional doping is predominantly based on ion implantation. It introduces the dopant atoms using high-energy ion bombardment.[3] The advantage of this technique is that the doping level and junction depth can be controlled independently.[4] However, this technique causes damage to the crystal structure and has difficulty with achieving ultrashallow doping.[5] The latter in particular plays a critical role in the downscaling of device dimensions.[6] Alternative doping techniques have been introduced including in situ chemical vapor deposition, solid source dotation, and proximity doping.[7] Very recently silicon nanoparticles doped with boron have been shown to effectively dope silicon wafers up to 10^{21} cm^{-3}.[8] Monolayer doping (MLD) is a promising alternative that was pioneered by Javey and co-workers.[9] MLD utilizes the hydrosilylation reaction to covalently bond dopant-containing molecules onto a hydrogen-terminated silicon surface.[10−14] The dopants are then driven into silicon by high-temperature annealing. MLD avoids crystal damage and offers the capability for ultrashallow doping and for doping 3-D structures.[15,16]

In semiconductor technology, silicon is doped in the range of 10^{15} to 10^{21} cm^{-3} to achieve desired electrical properties. Initially reported doping levels of silicon using MLD have been on the order of 10^{20} cm^{-3}. We have recently reported an MLD process based on mixed monolayers to achieve lower doping levels in a controlled manner.[17] In this concept, the doping precursor is mixed with an alkene that does not contain the dopant, and this mixture is grafted onto the silicon surface by hydrosilylation. Varying the mixing ratio has resulted in an effective tuning of the doping level in silicon. Yet, the nature of this mixing process limits its application to lower doping levels only. Yerushalmi and co-workers have recently proposed monolayer contact doping.[18] By this method, the doping precursor is first grafted onto a donor substrate by hydrosilylation, and this substrate is then brought into contact with the target substrate. A subsequent high-temperature annealing step is used to drive the dopant atoms into both the donor and target substrates. By repeating the hydrosilylation-contact-

Received: September 22, 2015
Accepted: November 23, 2015
Published: November 23, 2015

ACS Publications © 2015 American Chemical Society

annealing cycle on the same target substrate, higher levels of phosphorus doping have been achieved.

Here we demonstrate a different approach to achieve higher doping levels. We designed and used alkene molecules that carry a carborane cluster. Using these molecules with their naturally high content of boron in MLD, higher doping levels in silicon can be achieved readily in a single grafting and annealing process. This makes the technique attractive when a higher doping level is required while minimizing the thermal budget.

■ RESULTS AND DISCUSSION

We followed the MLD process as previously described (Figure 1A).[17] Three types of previously reported carborane derivatives were tested: ortho-carborane (CB-H_2), the monoallyl, monomethyl derivative CB-(Me, allyl),[19] and the bis-allyl derivative CB-$(allyl)_2$[20] (Figure 1B). All carborane derivatives contain 10 B atoms per molecule, intended to promote high boron doping levels. The allyl groups of CB-(Me, allyl) and CB-$(allyl)_2$ allow reaction with hydrogen-terminated silicon and therefore the covalent grafting of the adsorbates onto the surface. CB-H_2 lacks such a reactive group and is therefore used as a control. Allylboronic acid pinacol ester (ABAPE) has been used previously[17] and serves here as a comparative control representing an adsorbate that has only a single B atom.

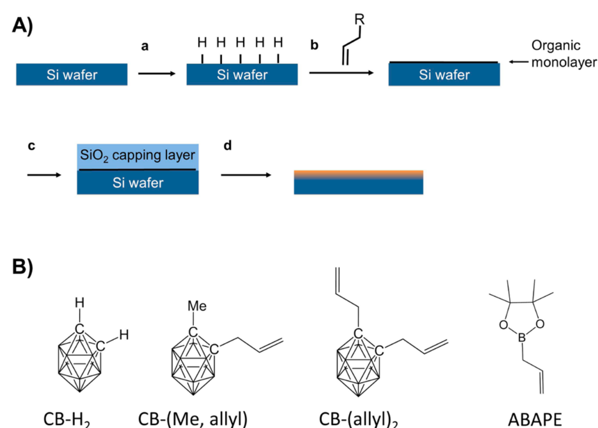

Figure 1. (A) Monolayer doping process: (a) wet etching of native SiO_2 with dilute aqueous HF yields the H-terminated silicon surface; (b) grafting of dopant molecules using hydrosilylation; (c) SiO_2 capping layer is sputtered onto the silicon surface with monolayers; (d) a spike annealing and removing of the capping layer results in a surface junction. (B) Structures of the carborane derivatives and the allylboronic acid pinacol ester (ABAPE).

The MLD process is schematically shown in Figure 1A. Silicon substrates were cleaned and etched with 1% HF to remove the native oxide. The carborane derivatives were grafted onto the H-terminated silicon surface by the hydrosilylation reaction. X-ray photoelectron spectroscopy (XPS) was performed to study the extent of functionalization. Boron, carbon, oxygen and silicon were quantified to determine the atomic concentrations of these elements. The results are summarized in Table 1. Samples functionalized with CB-(Me, allyl) and CB-$(allyl)_2$ showed significantly higher amounts of boron than the ones with compound CB-H_2 and ABAPE. Carbon values shown in Table 1 are higher than arising from the adsorbates alone, which is attributed to adventitious carbon as observed before.[17] Nevertheless, boron-to-carbon ratios were significantly higher for the former two cases. Figure 2 shows the XPS spectra of silicon substrates modified with monolayers of the three carborane derivatives. A B1*s* peak at about 189.6 eV is visible for the CB-(Me, allyl) and CB-$(allyl)_2$. No boron signal is observed for the CB-H_2. When comparing the boron contents of the monolayers of CB-(Me, allyl) and CB-$(allyl)_2$ with that of ABAPE, the former two show 8−10 times more boron than for ABAPE. This agrees favorably with the difference in the amount of boron atoms in the respective adsorbate molecules. Because CB-(Me, allyl) and CB-$(allyl)_2$ have similar structures and give similar boron contents at the surface, we used only CB-(Me, allyl) and ABAPE in subsequent analyses.

Table 1. XPS Atomic Percentages on Silicon after Monolayer Formation

Compd	B [%]	C [%]	B/C ratio	O [%]	Si [%]
CB-H_2	0.19	26.86	0.007	29.61	43.34
CB-(Me, allyl)	9.33	29.31	0.32	19.65	41.72
CB-$(allyl)_2$	10.25	43.88	0.23	15.66	30.21
ABAPE[a]	1.09	34.05	0.032		

[a] Values of this compound reported in ref 17.

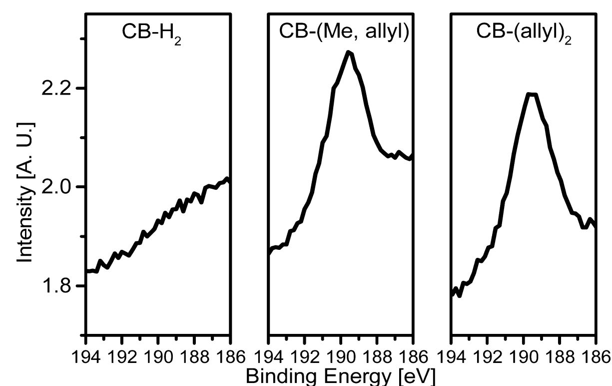

Figure 2. XPS B1*s* spectra of silicon substrates modified with CB-H_2, CB-(Me, allyl), and CB-$(allyl)_2$.

A SiO_2 capping layer was deposited on the monolayers of CB-(Me, allyl) and ABAPE, and these samples were annealed at three different temperatures. Boron profiles for the CB-(Me, allyl) annealed under these conditions and ABAPE samples annealed at 1000 °C for 6 s were measured by dynamic secondary ion mass spectrometry (D-SIMS) (Figure 3a). The junction depth as well as the doping concentration increase as the annealing temperature increases. The carborane sample annealed at 1000 °C showed a much higher doping concentration and deeper junction compared to the ABAPE sample annealed under the same conditions (Figure 3a). The total amount of boron (Figure 3b) showed a 7.3 times increase for the carborane sample (2.2×10^{13} cm^{-2}) compared to the ABAPE sample (0.30×10^{13} cm^{-2}). Considering a 10% error in the D-SIMS measurements, these numbers agree well with the observed difference in amounts of B present in the monolayers preceding annealing.

We also annealed a sample at 1000 °C for 15 s (Figure 3a,b). As expected, the total amount of boron increases compared to the annealing at 1000 °C for 6 s (Figure 3b). However, these results also indicate that the annealing time has a smaller impact on the dopant concentration than the annealing temperature. Varying the annealing temperature by 50 °C results in a significant change in both the highest doping concentration and

DOI: 10.1021/acsami.5b08952
ACS Appl. Mater. Interfaces 2015, 7, 27357−27361

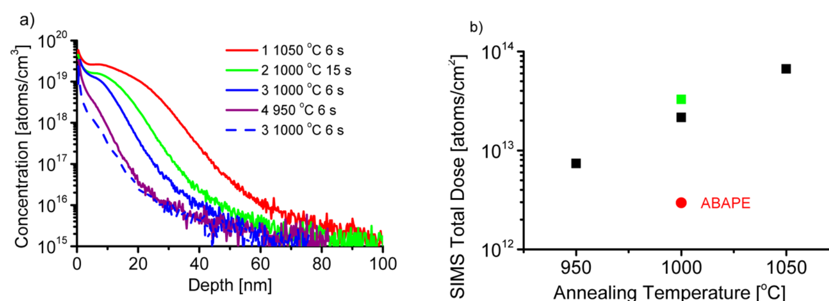

Figure 3. (a) D-SIMS profiles of boron for the samples made by MLD using CB-(Me, allyl) (solid lines) and ABAPE (dashed line), annealed at: (1) 1050 °C, 6 s (red); (2) 1000 °C, 15 s (green); (3) 1000 °C, 6 s (blue); and (4) 950 °C, 6 s (purple). (b) Total boron dose of samples made from CB-(Me, allyl) annealed for 6 s as a function of annealing temperature (■). Samples made from ABAPE annealed for 6 s (●) and from CB-(Me, allyl) annealed for 15 s (■) are also shown. All concentrations and total dose measurements have errors below 10%.

the total dopant dose. On the other hand, increasing the annealing time by 2.5x changes the total doping dose only slightly, and almost no change in the highest doping concentration was observed. Furthermore, we observed a plateau in the doping profiles near the surface for samples annealed at 1000 °C and 1050 °C. This kink-and-tail behavior is attributed to the solid solubility of boron in silicon.[21] As the solubility of B is related to the temperature, the highest level of doping is achieved at the highest annealing temperature. A high annealing temperature is thus needed when a high doping concentration is desired. However, the increased diffusivity of dopants at higher temperatures makes it more challenging to achieve shallow doping.

The sheet resistance (R_s) of the samples was measured subsequently using the four-point Van der Pauw method. The measured sheet resistances for the carborane and ABAPE samples are shown in Figure 4. The R_s values of the ABAPE samples were 17, 20, 13, and 3.1 times higher than the carborane samples annealed at the same conditions. The significantly lower R_s values of the carborane samples clearly indicate increased dopant concentrations in these samples compared to ABAPE. Since the conductivity of a sample is inversely related to the sheet resistance, the roughly 1 order of magnitude higher conductivities obtained by the carborane samples agrees well with the 10 times higher boron content in the adsorbate and its subsequent monolayers. These results also indicate that despite the high thermal stability of carboranes, the extent of the incorporation of the boron atoms within the crystal lattice is similar as for previously observed adsorbates under the same annealing conditions. Further on, atomic force microscopy measurements of the surface morphology of the silicon wafer before and after the doping cycle revealed no considerable modifications (Figure S1).

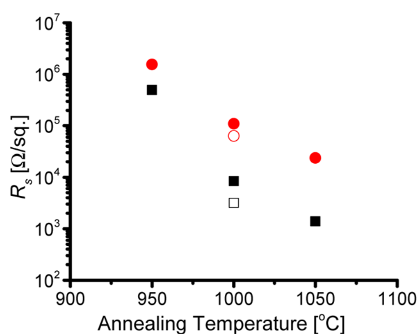

Figure 4. Four-point Van der Pauw measurements of the sheet resistance (R_s) on the samples prepared using CB-(Me, allyl) (square, ■ and □) and ABAPE (circle, ● and ○) as a function of the annealing temperature. The solid squares and circles (■ and ●) indicate the samples annealed for 6 s, and the hollow square and circle (□ and ○) indicate the samples that were annealed for 15 s. Errors for the carborane samples were found to be below ±1% except for the sample annealed at condition 4, which had an error of 22%. For the ABAPE samples, the errors were found to be below ±4% except for the sample annealed at condition 3, which had an error of 13%.

We further studied the correlation between the annealing process and the resulting doping level. Due to the short annealing time and comparable time scales of temperature ramping, it is difficult to make a direct comparison between the different annealing conditions. To solve this issue, we employed a thermal budget[22] evaluation, which takes into account the temperature dependence of the diffusivity. According to Fick's law the diffusivity of dopant atoms is defined as

$$D = D_0 \exp\left(\frac{-E_a}{k_B T}\right)$$

where E_a is the activation energy for diffusion, k_B is Boltzmann's constant, and T is the temperature. We calculated the thermal budget for each diffusion condition which is defined as the multiplication of D and time (t).[23] Given the fact that the temperature also varies with time during the annealing process, the thermal budget can be calculated as

$$Thermal\ Budget = D_0 \int \exp\left(-\frac{E_a}{k_B T(t)}\right) dt$$

Using the temperature ramping curve followed during the annealing process, we performed numerical calculations of the thermal budget for each annealing condition. The thermal budget arises from a temperature ramp-up, a hold phase, and a ramp-down. The separate contributions of these phases to the thermal budget are shown in Figure 5. The ramp-up and ramp-down phases contribute to about 10% each to the total thermal budget. These become more important when shorter annealing times are used, and therefore the thermal budget calculation as presented here is most important when evaluating conditions for ultrathin doping layers.

Figure 5b shows the total dopant dose derived from D-SIMS and the inverse of the sheet resistance ($1/R_s$) of the samples as a function of the thermal budget. The nearly linear dependence of the sheet resistance (R_s) and the SIMS dopant dose on the thermal budget indicates that the thermal process determines the amount of boron that has diffused into the silicon. This also

DOI: 10.1021/acsami.5b08952
ACS Appl. Mater. Interfaces 2015, 7, 27357−27361

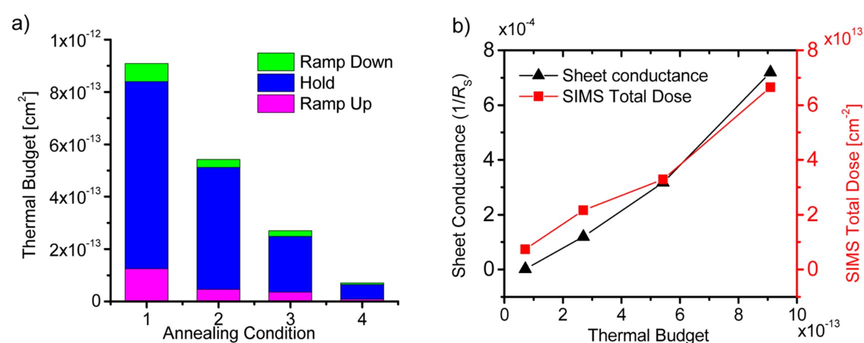

Figure 5. (a) Thermal budget of the four annealing conditions: (1) 1050 °C, 6 s; (2) 1000 °C, 15 s; (3) 1000 °C, 6 s; (4) 950 °C, 15 s. Note that the thermal budgets of ramp-up, hold, and ramp-down phases are shown separately. (b) Inverses of the sheet resistance ($1/R_s$) and total dopant doses derived from SIMS are also plotted to show the correlation of these with the thermal budget.

implies that with the CB-(Me, allyl) used in this study, the amount of boron at the silicon surface before the annealing step can be seen as an infinite source. The highest possible doping level is hence dominated by the thermal annealing step. As discussed above, the surface concentration is limited by the annealing temperature. These factors indicate that by changing the annealing temperature and time, the doping concentration and dose can be controlled independently to some extent.

■ CONCLUSION

A novel strategy for achieving high p-doping levels in Si by monolayer doping has been presented, using carborane molecules as a rich source of boron atoms. The XPS measurements indicate about ten times more boron atoms presented on the carborane-modified monolayers compared to ABAPE samples, in line with the difference in B atoms present in these molecules. D-SIMS and sheet resistance measurements also indicated a ten times increase in the doping dose under the same annealing conditions when comparing carborane and ABAPE samples. A thermal budget evaluation indicated good correlations between the SIMS dose and the conductivity, on the one hand, and the thermal budget, on the other hand, indicating a good control over the dopant dose by the thermal annealing conditions, also for spike anneal conditions.

■ METHODS AND MATERIALS

Compounds preparation. CB-H_2 (1,2-$C_2B_{10}H_{12}$) was supllied by Katchem Ltd. (Prague) and used as received. CB-(Me, allyl) (1-CH_3-2-$CH_2CH{=}CH_2$-1,2-$C_2B_{10}H_{10}$) and CB-(allyl)$_2$ (1,2-($CH_2{-}CH{=}CH_2$)$_2$-1,2-$C_2B_{10}H_{10}$) were prepared according to the literature.[19,20]

Monolayer formation. The samples were prepared using the same method as previously published.[17] The adsorbates were dissolved in mesitylene and the solutions were degassed using the freeze−pump−thaw method. A lightly n-doped silicon ⟨100⟩ wafer (resistivity >10 kΩ cm) was diced into 1 × 1 cm pieces, cleaned in acetone by sonication for 10 min, followed by a Piranha solution for 30 min. A dip in 1% HF for 1 min removed the native oxide and yielded a hydrogen-terminated Si surface. The silicon substrate and the degassed solution were put into a reaction flask in a nitrogen glovebox. The flask was then heated to 180 °C in an oil bath overnight at a constant nitrogen flux. After the reaction the samples were taken out and rinsed with ethanol, acetone, and Milli-Q water. Samples were then sonicated in acetone for 10 min to remove any physisorbed material.

Capping layer deposition and annealing. 100 nm of SiO_2 was sputtered onto monolayer-modified samples using a custom-built sputtering system. The chamber was backfilled with 1 sccm of oxygen to achieve stoichiometric SiO_2 layers. The annealing was performed using a Solaris 150 rapid thermal annealing system. The temperature ramp-up and ramp-down rates were 75 °C/s and 125 °C/s, respectively. The times given for the annealing conditions correspond to the total times including ramp-up, holding, and ramp-down phases, and the temperature was monitored at all stages.

SIMS measurements. In-diffused samples were first etched in HF to remove the capping layer and then cleaned with Piranha. SIMS measurements were performed by Jurgen van Berkum, Philips Innovation Service. Depth profiles were recorded using a Cameca IMS 6f system with 3 keV O_2^+ primary ions in positive mode. Secondary ions of ^{11}B and ^{31}P were detected. The measured ^{11}B concentration was converted to total boron coverage using the known isotopic ratio. The measurement chamber was backfilled with O_2. Quantification and depth calibration were based on reference samples with known profiles.

■ ASSOCIATED CONTENT

Supporting Information

The Supporting Information is available free of charge on the ACS Publications website at DOI: 10.1021/acsami.5b08952.

AFM images of undoped and doped silicon surfaces (PDF)

■ AUTHOR INFORMATION

Corresponding Authors

*E-mail: t.kudernac@utwente.nl.

*E-mail: j.huskens@utwente.nl.

Notes

The authors declare no competing financial interest.

■ ACKNOWLEDGMENTS

We would like to thank Janneke Veerbeek and Wouter Vijselaar for fruitful discussions. L.Y. acknowledges the China Scholarship Council for financial support. This work was supported by projects MAT2013-47869-C4-P2, CTQ2013-44670-R and by Generalitat de Catalunya (2014/SGR/149). A.G.-C. acknowledges the CSIC for the JAE-DOC contract.

■ REFERENCES

(1) Peercy, P. S. The Drive to Miniaturization. *Nature* **2000**, *406*, 1023−1026.

(2) Lundstrom, M. Moore's Law Forever? *Science* **2003**, *299*, 210−211.

(3) Jones, E. C.; Ishida, E. Shallow Junction Doping Technologies for Ulsi. *Mater. Sci. Eng., R* **1998**, *24*, 1−80.

(4) Aleman, M.; Rosseel, E.; Van Wichelen, K.; Pawlak, B. J.; Janssens, T.; Dross, F.; Posthuma, N. E.; Poortmans, J. In Ion Implantation as a Potential Alternative for the Formation of Front Surface Fields for Ibc Silicon Solar Cells. *35th IEEE Photovoltaic*

Specialists Conference, Honolulu, HI, June 20−25, 2010;, Honolulu, HI, 2010; pp 1291−1294.

(5) Stolk, P. A.; Gossmann, H. J.; Eaglesham, D. J.; Jacobson, D. C.; Rafferty, C. S.; Gilmer, G. H.; Jaraiz, M.; Poate, J. M.; Luftman, H. S.; Haynes, T. E. Physical Mechanisms of Transient Enhanced Dopant Diffusion in Ion-Implanted Silicon. *J. Appl. Phys.* **1997**, *81*, 6031−6050.

(6) Lee, J. W.; Sasaki, Y.; Cho, M. J.; Togo, M.; Boccardi, G.; Ritzenthaler, R.; Eneman, G.; Chiarella, T.; Brus, S.; Horiguchi, N.; Groeseneken, G.; Thean, A. Plasma Doping and Reduced Crystalline Damage for Conformally Doped Fin Field Effect Transistors. *Appl. Phys. Lett.* **2013**, *102*, 223508.

(7) Elbersen, R.; Vijselaar, W.; Tiggelaar, R. M.; Gardeniers, H.; Huskens, J. Fabrication and Doping Methods for Silicon Nano- and Micropillar Arrays for Solar-Cell Applications: A Review. *Adv. Mater.* **2015**, DOI: 10.1002/adma.201502632.

(8) Gao, Y.; Zhou, S.; Zhang, Y.; Dong, C.; Pi, X.; Yang, D. Doping Silicon Wafers with Boron by Use of Silicon Paste. *J. Mater. Sci. Technol.* **2013**, *29*, 652−654.

(9) Ho, J. C.; Yerushalmi, R.; Jacobson, Z. A.; Fan, Z.; Alley, R. L.; Javey, A. Controlled Nanoscale Doping of Semiconductors Via Molecular Monolayers. *Nat. Mater.* **2008**, *7*, 62−67.

(10) Li, Y.; Calder, S.; Yaffe, O.; Cahen, D.; Haick, H.; Kronik, L.; Zuilhof, H. Hybrids of Organic Molecules and Flat, Oxide-Free Silicon: High-Density Monolayers, Electronic Properties, and Functionalization. *Langmuir* **2012**, *28*, 9920.

(11) Scheres, L.; Giesbers, M.; Zuilhof, H. Organic Monolayers onto Oxide-Free Silicon with Improved Surface Coverage: Alkynes Versus Alkenes. *Langmuir* **2010**, *26*, 4790−4795.

(12) Scheres, L.; Arafat, A.; Zuilhof, H. Self-Assembly of High-Quality Covalently Bound Organic Monolayers onto Silicon. *Langmuir* **2007**, *23*, 8343−8346.

(13) Buriak, J. M. Organometallic Chemistry on Silicon and Germanium Surfaces. *Chem. Rev.* **2002**, *102*, 1271−1308.

(14) Buriak, J. M. Organometallic Chemistry on Silicon Surfaces: Formation of Functional Monolayers Bound through Si-C Bonds. *Chem. Commun.* **1999**, 1051−1060.

(15) Longo, R. C.; Cho, K.; Schmidt, W. G.; Chabal, Y. J.; Thissen, P. Monolayer Doping Via Phosphonic Acid Grafting on Silicon: Microscopic Insight from Infrared Spectroscopy and Density Functional Theory Calculations. *Adv. Funct. Mater.* **2013**, *23*, 3471−3477.

(16) Ho, J. C.; Yerushalmi, R.; Smith, G.; Majhi, P.; Bennett, J.; Halim, J.; Faifer, V. N.; Javey, A. Wafer-Scale, Sub-5 Nm Junction Formation by Monolayer Doping and Conventional Spike Annealing. *Nano Lett.* **2009**, *9*, 725−730.

(17) Ye, L.; Pujari, S. P.; Zuilhof, H.; Kudernac, T.; de Jong, M. P.; van der Wiel, W. G.; Huskens, J. Controlling the Dopant Dose in Silicon by Mixed-Monolayer Doping. *ACS Appl. Mater. Interfaces* **2015**, *7*, 3231−3236.

(18) Hazut, O.; Agarwala, A.; Amit, I.; Subramani, T.; Zaidiner, S.; Rosenwaks, Y.; Yerushalmi, R. Contact Doping of Silicon Wafers and Nanostructures with Phosphine Oxide Monolayers. *ACS Nano* **2012**, *6*, 10311−10318.

(19) González-Campo, A.; Vinas, C.; Teixidor, F.; Nuñez, R.; Sillanpää, R.; Kivekäs, R. Modular Construction of Neutral and Anionic Carboranyl-Containing Carbosilane-Based Dendrimers. *Macromolecules* **2007**, *40*, 5644−5652.

(20) González-Campo, A.; Nuñez, R.; Viñas, C.; Boury, B. Synthetic Approaches to the Preparation of Hybrid Network Materials Incorporating Carborane Clusters. *New J. Chem.* **2006**, *30*, 546−553.

(21) Hull, R. *Properties of Crystalline Silicon*; INSPEC: London, United Kingdom, 1999.

(22) Fair, R. B. Challenges to Manufacturing Submicron, Ultra-Large Scale Integrated-Circuits. *Proc. IEEE* **1990**, *78*, 1687−1705.

(23) Regner, J. An Analytical Approach to Quantify the Thermal Budget in Consideration of Consecutive Thermal Process Steps. *10th IEEE International Conference on Advanced Thermal Processing of Semiconductors - Rtp 2002* **2002**, 15−20.

DOI: 10.1021/acsami.5b08952
ACS Appl. Mater. Interfaces 2015, 7, 27357−27361